

Three-dimensional spatiotemporal nondiffracting parabolic cylinder beamsWenYe Zhong,¹ Wei-Ping Zhong^{2,*}, Milivoj Belić,³ Zhengping Yang,⁴ and Guofa Cai^{1,†}¹*School of Information Engineering, Guangdong University of Technology, Guangzhou 510006, China*²*Department of Electronic Engineering, Shunde Polytechnic, Guangdong Province, Shunde 528300, China*³*Texas A&M University at Qatar, 23874 Doha, Qatar*⁴*Department of Medical Science, Shunde Polytechnic, Guangdong Province, Shunde 528300, China*

(Received 1 June 2021; accepted 13 October 2021; published 15 November 2021)

In this paper, the propagation characteristics of three-dimensional spatiotemporal nondiffracting parabolic cylinder beams in free space are studied. From the (3+1)-dimensional paraxial wave equation, we obtain an exact solution by the method of separating variables. The solution is constructed using parabolic cylinder functions, described by the three optical mode numbers. The spatiotemporal intensity distribution of the parabolic cylinder beam at five times Rayleigh range with different mode parameters is presented analytically and simulated numerically. Our results indicate that the intensity distribution can be well controlled by adjusting the values of the three mode numbers. They are of great significance for improved understanding of the formation mechanism of parabolic cylinders and other nondiffracting beams.

DOI: [10.1103/PhysRevA.104.053514](https://doi.org/10.1103/PhysRevA.104.053514)**I. INTRODUCTION**

A nondiffracting optical beam is a beam whose transverse intensity distribution will not change in the process of beam propagation [1]. This kind of beams exhibit some unique properties, such as high intensity concentration of the light field, a small central spot, and, when encountering obstacles, the ability to restore the original intensity distribution. Because of these characteristics, nondiffracting beams have found applications in many fields, so many scholars continue to explore their peculiar properties. Due to nondivergence and high concentration of light intensity, such beams have been widely used in different fields, for example, in optical manipulation [2], imaging [3], scanning [4], communications [5], and so on. Nondiffracting beams often also accelerate [6].

In 1987, Durnin *et al.* first proposed a nondiffracting Bessel beam in free space, which is a special solution of scalar paraxial wave equation in cylindrical coordinates [7]. The paraxial wave equation can have variables separated in 11 kinds of orthogonal coordinate systems, but only in Cartesian, cylindrical, elliptic, and parabolic cylindrical coordinates, can the nondiffracting wave solution be obtained. The solutions obtained in these four coordinate systems, corresponding to different Bessel [7], cosine [8], Mathieu [9], and parabolic beams [10], form a family of nondiffracting beams. In 2000, Salo *et al.* [11] put forward a method of representing the wave field of nondiffracting light, by which any monochromatic nondiffracting wave can be described as the superposition of all plane waves whose wave vectors are located on a cone. Bessel beams have been researched a lot since they were put forward several decades ago, but the other three kinds of beams have been studied less. The nondiffracting Mathieu

beam was reported by Gutierrez-Vega *et al.* and in the following year, the beam was confirmed by experiment [12]. In 2004, Bandres *et al.* introduced the parabolic beam [13]. In 2005, López Mariscal *et al.* [14] observed the parabolic beam in the laboratory. In recent years, researchers have continued to explore nondiffracting beams, especially their intensity distributions. Interestingly, Garcés-Chávez *et al.* [15] applied a self-reconstructing beam to multilayer particle micromanipulation, which brought the application of nondiffracting beams into a new era.

The essential effect in optical wave packet propagation is beam diffraction, which is one of the most difficult problems to treat in physical optics. In diffraction theory, due to mathematical difficulties, there are few exact solutions, and in most cases, approximate methods must be used. The exploration of spatiotemporal optical wave packets is obviously intertwined with the development of materials science needs and the formation of adequate experimental abilities. In recent years, in the field of three-dimensional (3D) spatiotemporal beams, various materials and technologies have been found to meet these needs. In 2001, Eisenberg *et al.* [16] studied the propagation of beams in planar fused silica waveguides. It was found that the optical pulse underwent spatiotemporal self-focusing and formed a stable beam; in 2010, Minardi *et al.* [17] fabricated a waveguide array using silicon fluoride glass material. The optical pulses with 0.4 milliwatt (mW) intensity, 1550 nm wavelength, and 170 fs pulse width were coupled into a waveguide array, and a three-dimensional spatiotemporal beam was obtained at the output. With the further development of optical technology and materials, in the near future it will hopefully be possible to experimentally confirm the 3D spatiotemporal nondiffracting parabolic cylinder beams obtained theoretically in this paper.

Here, the (3+1)-dimensional paraxial wave equation will be transformed into three independent partial differential equations in time and space domains, using the separation of

*zhongwp6@126.com

†caiguofa2006@gdut.edu.cn

variables method. By solving three independent partial differential equations, we obtain their exact solutions, which are constructed by the parabolic cylinder functions and described by three discrete numbers. We denote these three parameters as the optical mode numbers, in analogy to the usual notation of wave functions and eigenvalues in the Schrödinger equation of quantum mechanics. When different mode numbers are selected, the intensity of the nondiffracting beam acquires different spatiotemporal distributions. In order to prove the validity and stability of the analytical solution, we take a specific analytical solution as an initial condition and use the split-step beam propagation method to numerically simulate its evolution according to the (3+1)-dimensional paraxial wave equation. The results show that the analytical solution is consistent with the numerical calculation.

II. OUR MODEL AND ITS EXACT SOLUTION

When a three-dimensional (3D) spatiotemporal nondiffracting beam propagates in free space, its light field $u(z, x, y, \tau)$ along the propagation z direction satisfies the following normalized (3+1)D paraxial wave equation [18–20],

$$i \frac{\partial u}{\partial z} + \frac{1}{2} \left(\frac{\partial^2 u}{\partial x^2} + \frac{\partial^2 u}{\partial y^2} + \frac{\partial^2 u}{\partial \tau^2} \right) = 0, \quad (1)$$

where x and y are the transverse rectangular coordinates, and τ represents the retarded time in the frame of reference moving with the optical pulse [18–20]. Since Eq. (1) involves three spatial and one temporal domain, we denote it as a (3+1)D spatiotemporal wave equation. To obtain an exact beam solution of Eq. (1), we assume that the trial solution is of the form

$$u(z, x, y, \tau) = \frac{q_0 A^3(z)}{q(z)} X(z, x) Y(z, y) T(z, \tau) \times e^{i \frac{x^2 + y^2 + \tau^2}{2} \left[\frac{1}{q(z)} + \frac{1}{2\chi^2(z)} \right]}, \quad (2)$$

where $X(z, x)$, $Y(z, y)$, and $T(z, \tau)$ are components in the x , y , and τ directions, respectively; $A(z)$ is a physical quantity introduced to normalize the wave function; $q(z) = z - iz_R$, $q_0 = q(z=0) = -iz_R$ with z_R being the Rayleigh range of a beam, which is also the basic unit used to measure the length along the propagation direction z of the parabolic cylinder beam; $\chi(z)$ is the z -dependent scaling factor, to be determined. To find the parabolic cylinder nondiffracting solution of Eq. (1), we resort to the separation of variables method. By directly substituting Eq. (2) into Eq. (1), one gets three independent equations in the space domain and time. For example, one discovers an equation for the $X(z, x)$ component of the nondiffracting beam, from the following three equations obtained in the substitution,

$$\frac{\partial \chi^2}{\partial z} - \frac{2\chi^2}{q} = 1, \quad (3)$$

$$\frac{2i\chi^2}{A} \frac{\partial A}{\partial z} + \frac{i}{2} + i \frac{\chi^2}{3q} - n - \frac{1}{2} = 0, \quad (4)$$

$$\frac{\partial^2 X}{\partial \Omega^2} + \left(n + \frac{1}{2} - \frac{\Omega^2}{4} \right) X = 0, \quad (5)$$

where n is a non-negative integer, which we call the mode number of the beam component in the x direction, and $\Omega(z, x) = \frac{x}{\chi(z)}$. By solving the first-order partial differential Eq. (3), one obtains an expression for the scaling factor in the form $\chi^2 = -q$. Substituting this expression into Eq. (4), we find that the solution of Eq. (4) is $A(z) = A_0(z_R + iz)^{-\frac{i}{12}(i-3-6n)}$, where $A_0 = A(z=0)$. When the normalized amplitude of the initial condition is assumed as $A(z=0) = 1$, it is easy to get $A_0 = (z_R)^{\frac{i}{12}(i-3-6n)}$. Obviously, Eq. (5) is the standard Weber differential equation [21], which explains the choice of the trial solution. The general solution of Eq. (5) can be written as $F(\Omega) = D_n(\Omega)$, where $D_n(\Omega)$ is the parabolic cylinder function. Therefore, the component $X(z, x)$ of the nondiffracting beam in the x direction can be expressed as

$$X(z, x) = (z_R)^{\frac{i}{12}(i-3-6n)} (z_R + iz)^{-\frac{i}{12}(i-3-6n)} \times D_n \left(\frac{x}{iz_R - z} \right) e^{i \frac{x^2}{4(z-iz_R)}}. \quad (6)$$

One similarly obtains the expressions of nondiffracting wave packets in the y and τ directions. By substituting these expressions into Eq. (2), one finds the total light field distribution,

$$u(z, x, y, \tau) = k_{nml}(z) D_n \left(\frac{x}{iz_R - z} \right) D_m \left(\frac{y}{iz_R - z} \right) \times D_l \left(\frac{\tau}{iz_R - z} \right) e^{i \frac{x^2 + y^2 + \tau^2}{4(z-iz_R)}}, \quad (7)$$

where

$$k_{nml}(z) = \frac{-iz_R}{z-iz_R} (z_R)^{\frac{i}{4}(i-3-2n-2m-2l)} (z_R + iz)^{-\frac{i}{4}(i-3-2n-2m-2l)}.$$

The parameters m and l are also two non-negative integers, the mode numbers of the optical wave packet in the y direction and the τ direction, respectively. Since the wave function of the light wave packet is constructed by three parabolic cylinder functions in Eq. (7), the wave packet is called the nondiffracting parabolic cylinder beam. Equation (7) describes the parabolic cylinder beam solution in free space, which is composed of three parabolic cylinder functions of different orders. The light intensity displays different characteristics in three-dimensional space and time. We discuss these characteristics in the next section.

III. ANALYSIS AND DISCUSSION

It can be seen from solution (7) that the properties of the nondiffracting wave packet crucially depend on the three mode numbers (n, m, l) and the three parabolic cylinder functions. In this section, we discuss the distribution of light intensity [$I = |u(z, x, y, \tau)|^2$] of various beams in the three-dimensional space and time. Without loss of generality, the temporal and spatial distributions of the wave packet at $z = 5z_R$ are discussed.

First of all, we take the modes with the same mode numbers to analyze, that is, the spatiotemporal distributions of the linear wave packet when $n = m = l$, at a certain propagation distance. When $n = m = l = 0$, the light field is in the ground

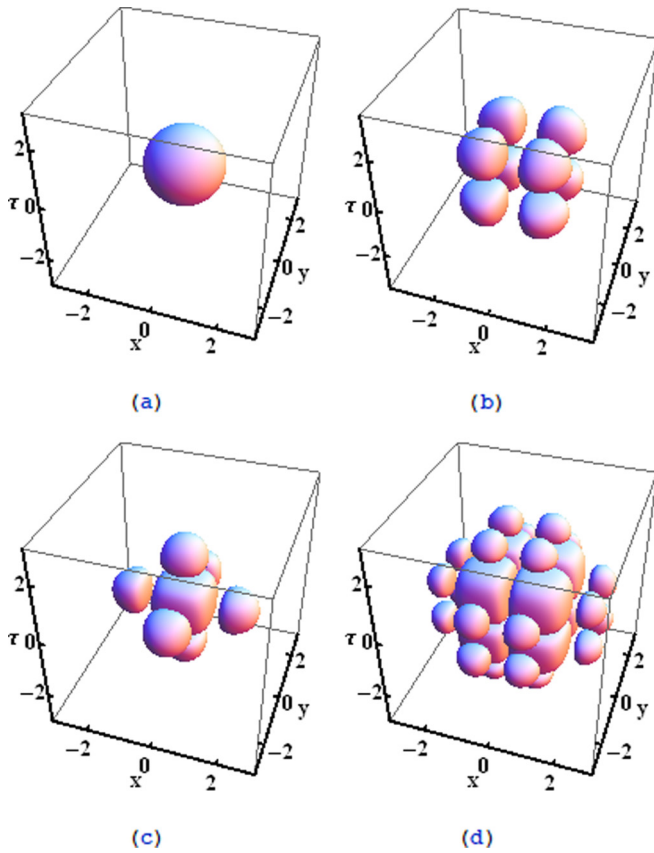


FIG. 1. Spatiotemporal intensity distribution with three identical mode numbers, at $z = 5z_R$. These numbers are (a) $n = m = l = 0$, (b) $n = m = l = 1$, (c) $n = m = l = 2$, and (d) $n = m = l = 3$, respectively.

state and has the lowest energy, displaying a Gaussian spherical packet, as shown in Fig. 1(a). Secondly, we discuss the spatiotemporal distribution of the intensity of three excited states still with the same mode numbers and energy larger than the ground state. When the three mode numbers are even or odd, the light intensity shows two different distributions in the three-dimensional space-time. These figures clearly exhibit the diversity of basic nondiffracting light waves in this model. It is worth noting that if three identical mode numbers are even, solution (7) describes a wave with nonzero light intensity at the central position $(x, y, \tau) = (0, 0, 0)$. We call it a Gaussian linear wave packet. Figure 1(c) is a typical example with $n = m = l = 2$. For higher excited states, the spatiotemporal distribution of nondiffracting waves is more complex, which is not shown here. Generally speaking, this kind of light wave packet has a large cube-shaped structure at $(x, y, \tau) = (0, 0, 0)$ and several smaller ellipsoids around it; there exist overall $(2n + 1)$ structures in the packet. On the other hand, if the three identical mode numbers are selected as odd, the cubic packet at the central position $(x, y, \tau) = (0, 0, 0)$ disappears and the light intensity is zero there, which is shown in Figs. 1(b) and 1(d). The nondiffracting wave packet consists of $2(n + 1)^2$ smaller structures in that case.

When one of the three mode numbers is zero and the other two are the same but nonzero, the beam intensity distribution displays a planar structure. Figures 2 and 3 show two typical

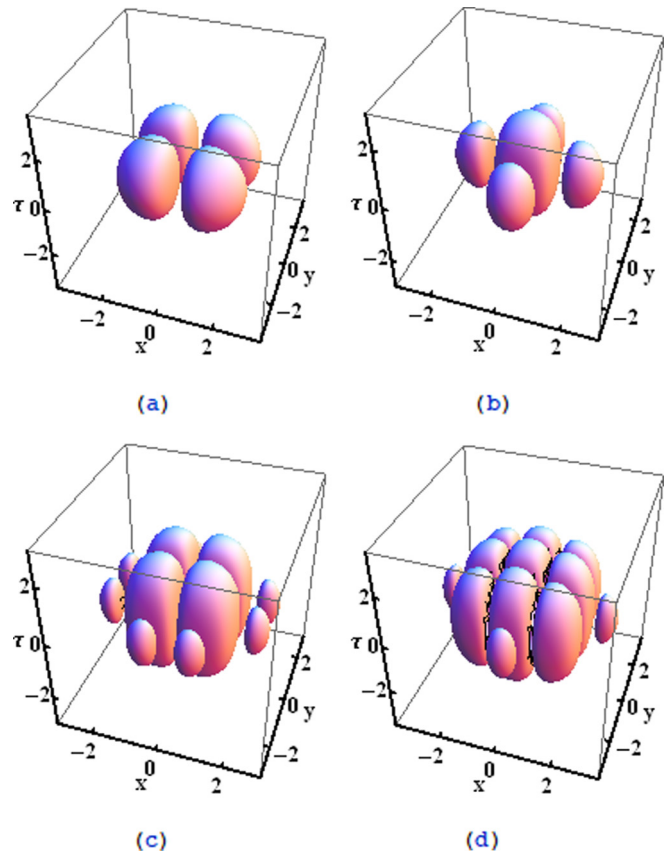


FIG. 2. Spatiotemporal intensity distributions with a zero mode number in the τ direction and two identical but nonzero discrete numbers at $z = 5z_R$. (a) $(n, m, l) = (1, 1, 0)$, (b) $(n, m, l) = (2, 2, 0)$, (c) $(n, m, l) = (3, 3, 0)$, and (d) $(n, m, l) = (4, 4, 0)$.

examples. In Fig. 2, the mode number in the τ direction is zero, and all structures lie in the x - y plane. The nondiffracting wave packets corresponding to the even numbers with $n = m$ are the already known Gaussian distributions described above in Figs. 1(a) and 1(c), as shown now in Figs. 2(b) and 2(d). In Fig. 2(b), we take mode numbers as $(n, m, l) = (2, 2, 0)$; in the middle position, there is a large ellipsoidal pulse distributed along the τ axis, which is symmetrically surrounded by four similar small ellipsoids. Further, if we increase the mode numbers from $(n, m, l) = (2, 2, 0)$ to $(n, m, l) = (4, 4, 0)$, these ellipsoids display a new arrangement, which is shown in Fig. 2(d). It is seen that the nondiffracting beam is composed as a two-dimensional (2D) layer of three kinds of ellipsoids, distributed along the τ direction. One ellipsoid in the middle position carries the largest amount of energy, surrounded by eight smaller ellipsoids with less energy, and the outermost layer is composed of four ellipsoids with the smallest energy. We can simply describe this kind of nondiffracting beam, as composed of $(n - 1)$ kinds of ellipsoids, with the total number $(4n - 3)$ of ellipsoids in the x - y plane.

To analyze the nondiffracting structures with odd mode numbers for $n = m$, solution (7) displays a different form from that discussed above. When the mode number $l = 0$ is chosen, the remaining two identical odd mode numbers are the parameters that affect the beam, and they play an important role in the spatiotemporal distribution. In fact, as

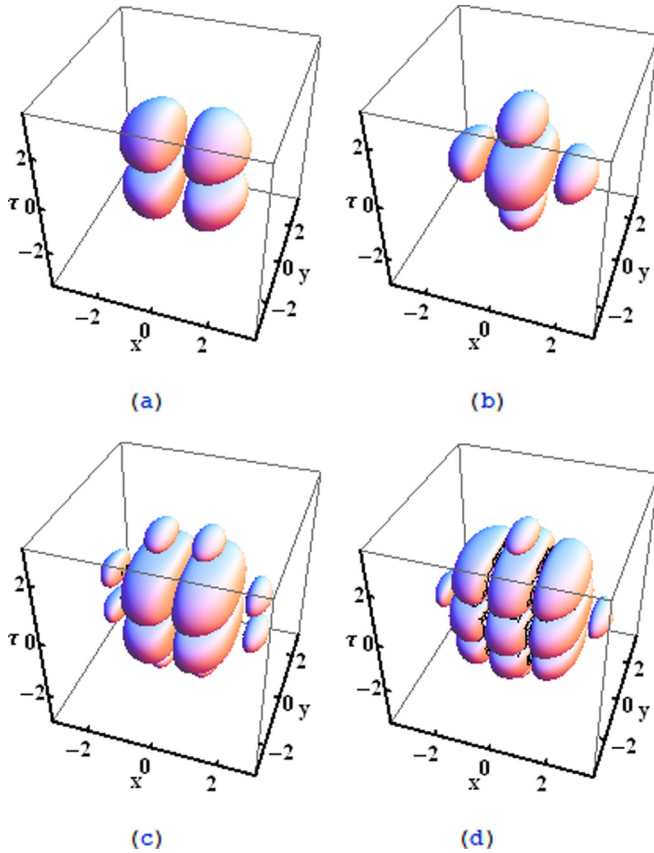


FIG. 3. Spatiotemporal beam patterns with $m = 0$ and two identical but nonzero discrete numbers at $z = 5z_R$. (a) $(n, m, l) = (1, 0, 1)$, (b) $(n, m, l) = (2, 0, 2)$, (c) $(n, m, l) = (3, 0, 3)$, and (d) $(n, m, l) = (4, 0, 4)$.

described in the previous paragraph, when $n = m = 1$, the four ellipsoids of the beam are distributed in the x - y plane, as shown in Fig. 2(a). On the other hand, considering a more complex case such as $n = m = 3$, the distribution of ellipsoids is shown in Fig. 2(c). It can be seen in the figure that the nondiffracting beam consists of two kinds of ellipsoids, the inner layer containing four ellipsoids with higher energy, and the outer layer consisting of eight ellipsoids with lower energy. Generally speaking, this type of beam is constructed by n types of ellipsoids, and contains $4n$ ellipsoids overall.

In order to further illustrate the above structures, we select the mode number with zero ($m = 0$) in the y direction and the same nonzero ($n = l \neq 0$) in the other two directions. Figure 3 shows the resulting distribution. By the way, it is not difficult to explain why Gaussian and non-Gaussian distributions are formed the way they are. When the mode number is zero or even, the value of the parabolic cylinder function reaches the maximum at the center position, so the nondiffracting wave packet forms a Gaussian beam [22]. For odd mode numbers, the value of the parabolic cylinder function at the center position is zero, which results in zero beam intensity at that position.

Because solution (7) contains three parabolic cylinder functions which are described by three non-negative integer mode numbers, the nondiffracting beams show abundant localized structures. To discuss more complex profiles,

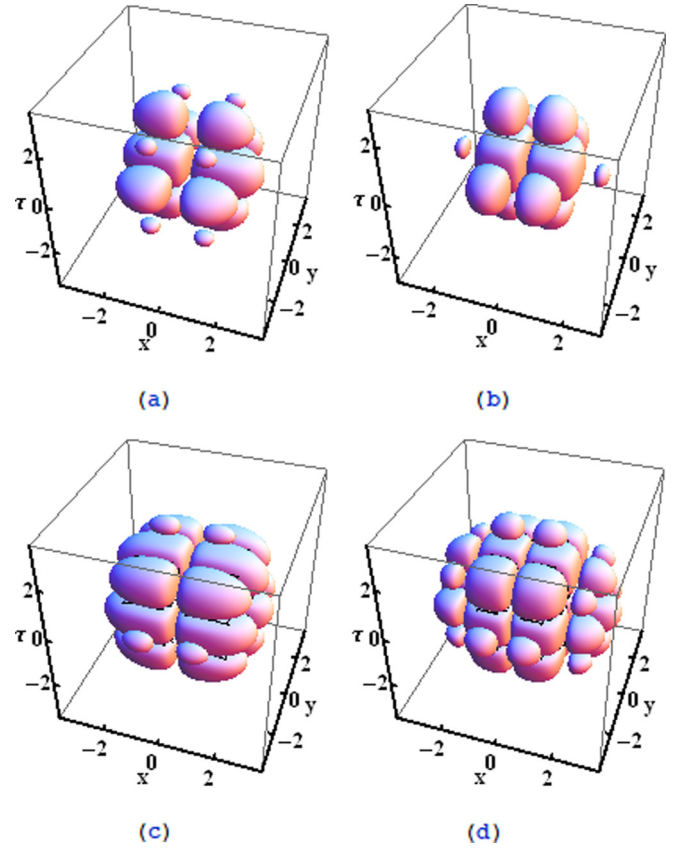


FIG. 4. Intensity profiles with two equal even numbers and one odd mode number at $z = 5z_R$. The three numbers are (a) $(n, m, l) = (1, 2, 2)$, (b) $(n, m, l) = (3, 2, 2)$, (c) $(n, m, l) = (1, 4, 4)$, and (d) $(n, m, l) = (3, 4, 4)$.

we take two equal even and one odd mode number, as an example. First, the three mode numbers are chosen as $(n, m, l) = (1, 2, 2)$. According to the shape, we call it the necklace ring structure, with the largest ellipsoid surrounded by eight adjacent large and small pearls in the vertical plane, and there are two rings along the x direction, as displayed in Fig. 4(a). When $(n, m, l) = (3, 2, 2)$ is selected, a large ellipsoid is surrounded by four smaller ellipsoids in the vertical plane, and there exist four rows in the x direction. The leftmost and rightmost appear as small pearls, which are shown in Fig. 4(b). Next, we take $(n, m, l) = (1, 4, 4)$ in solution (7) to obtain the superposition ellipsoidal structure shown in Fig. 4(c). As can be seen, there are two rows along the x direction and three layers in the vertical direction. Three ellipsoids are superposed along the τ axis, and the outermost layer is surrounded by the four smallest ellipsoids. Finally, a more complex case $(n, m, l) = (3, 4, 4)$ is shown and its structure exhibited in Fig. 4(d).

IV. COMPARISON WITH NUMERICAL SIMULATION

Finally, it should be stressed that the correctness and the stability of the analytical solution (7) of the (3+1)-dimensional paraxial wave equation (1) represent important problems. They are addressed in this section. To achieve these goals, we perform a direct numerical simulation of Eq. (1),

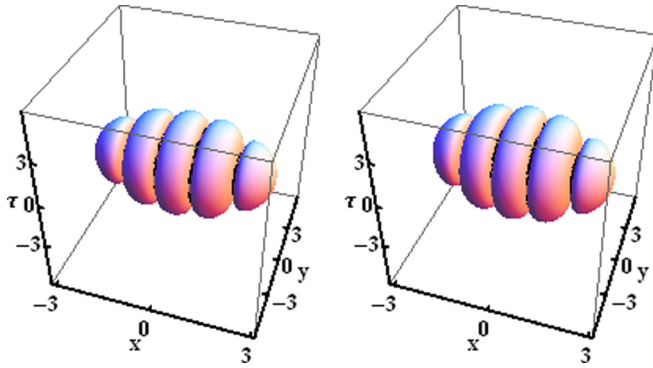


FIG. 5. Comparison of the analytical solution (7) with the numerical simulation, for mode numbers $(n, m, l) = (4, 0, 0)$ at $z = 5z_R$. The left panel is the analytical solution (7) and the right panel is the numerical simulation of Eq. (1).

with the initial condition at $z = 0$ chosen from the analytical solution (7). This is done with the aid of the split-step beam propagation method [23,24]. An example of such numerical simulation is displayed in Fig. 5, with the three mode numbers chosen as $(n, m, l) = (4, 0, 0)$. In the figure, the stable numerical solution at $z = 5z_R$ is compared with the analytical solution. One can see that the numerical simulation (the right panel) looks very much like the numerical solution (the left panel). In addition, numerical calculation indicates no collapse, as is expected in this linear problem. Indeed, stable propagation over five Rayleigh lengths is observed. This example also confirms that the analytical solution is consistent with the numerical calculation. Similar behavior is observed for other initial conditions.

V. CONCLUSIONS

This paper presents a way of generating three-dimensional spatiotemporal nondiffracting parabolic cylinder beams. By using the method of separating variables, we find exact localized solutions of the (3+1)-dimensional normalized spatiotemporal paraxial wave equation. These solutions are constructed by three parabolic cylinder functions and are described by three optical mode numbers. Several nondiffracting local wave patterns are displayed by properly choosing these numbers. The results show that the beam intensity can be easily controlled by adjusting the values of the three numbers and are of great significance for an improved understanding of the formation mechanism of parabolic cylinder beams. It is a long-term task for researchers to explore new spatiotemporal solutions of the paraxial wave equation and construct new localized excitation structures. At the same time, we also look forward to the eventual experimental confirmation of the theoretical predictions made in this paper.

ACKNOWLEDGMENTS

This work was supported by the Natural Science Foundation of Guangdong, China, under Grant No. 2019A1515010749, and by Key projects of basic research and applied basic research in universities of Guangdong province, China, under Grants No. 2019GZDXM001 and No. 2021ZDZX1118. The work at the Texas A&M University at Qatar was supported by NPRP Project No. 11S-1126-170033 with the Qatar National Research Fund. This work was also supported in part by the Natural Science Foundation of China, under Grants No. 61801128 and No. 62071129.

-
- [1] J. Durnin, Exact solutions for non-diffracting beams. I. The scalar theory, *J. Opt. Soc. Am. A* **4**, 651 (1987).
 - [2] D. G. Grier, A revolution in optical manipulation, *Nature (London)* **424**, 810 (2003).
 - [3] S. Lee, B. Joo, P. J. Jeon, S. Im, and K. Oh, Columnar deformation of human red blood cell by highly localized fiber optic Bessel beam stretcher, *Bioomed. Opt. Express* **6**, 4417 (2015).
 - [4] P. J. Keller, A. D. Schmidt, A. Santella, K. Khairy, Z. Bao, J. Wittbrodt, and E. H. K. Stelzer, Fast, high-contrast imaging of animal development with scanned light sheet-based structured-illumination microscopy, *Nat. Methods* **7**, 637 (2010).
 - [5] M. McLaren, T. Mhlanga, M. J. Padgett, F. S. Roux, and A. F. Orbes, Self-healing of quantum entanglement after an obstruction, *Nat. Commun.* **5**, 3248 (2014).
 - [6] I. Caminer, R. Bekenstein, J. Nemirovsky, and M. Segev, Nondiffracting Accelerating Wave Packets of Maxwell's Equations, *Phys. Rev. Lett.* **108**, 163901 (2012).
 - [7] J. Durnin, J. J. Miceli, Jr., and J. H. Eberly, Diffraction-Free Beams, *Phys. Rev. Lett.* **58**, 1499 (1987).
 - [8] S. M. Wang, Q. Lin, and X. Q. Jiang, Cosine-Gauss beam, *Acta Photon. Sin.* **28**, 367 (1999) (in Chinese).
 - [9] J. C. Gutierrez-Vega, M. D. Iturbe-Castillo, and S. Chavez-Cerda, Alternative formulation for invariant optical fields: Mathieu beams, *Opt. Lett.* **25**, 1493 (2000).
 - [10] W.-P. Zhong, M. Belić, B. A. Malomed, T. Huang, and G. Chen, Accessible spatiotemporal parabolic-cylinder solitons, *J. Phys. B: At. Mol. Opt. Phys.* **46**, 075401 (2013).
 - [11] J. Salo, J. Fagerholm, A. Friberg, and M. Salomaa, Unified description of nondiffracting X and Y waves, *Phys. Rev. E* **62**, 4261 (2000).
 - [12] J. C. Gutierrez-Vega, M. D. Iturbe-Castillo, G. A. Ramirez, E. Tepichna, R. M. Rodriguez-Dagninob, S. Chavez-Cerda, and G. H. C. New, Experimental demonstration of optical Mathieu beams, *Opt. Commun.* **195**, 35 (2001).
 - [13] M. A. Bandres, J. C. Gutierrez-Vega, and S. S. Chavez-Cerda, Parabolic nondiffracting optical wave fields, *Opt. Lett.* **29**, 44 (2004).
 - [14] C. López Mariscal, M. A. Bandres, J. C. Gutiérrez-Vega, and S. Chávez-Cerda, Observation of parabolic nondiffracting optical fields, *Opt. Express* **13**, 2364 (2005).

- [15] V. Garcés-Chávez, D. McGloin, H. Melville, W. Sibbett, and K. Dholakia, Simultaneous micromanipulation in multiple planes using a self-reconstructing light beam, *Nature (London)* **419**, 145 (2002).
- [16] H. S. Eisenberg, R. Morandotti, Y. Silberberg, and S. Bar-Ad, Kerr Spatiotemporal Self-Focusing in a Planar Glass Waveguide, *Phys. Rev. Lett.* **87**, 043902 (2001).
- [17] S. Minardi, F. Eilenberger, Y. V. Kartashov, A. Szameit, and T. Pertsch, Three-Dimensional Light Bullets in Arrays of Waveguides, *Phys. Rev. Lett.* **105**, 263901 (2010).
- [18] W.-P. Zhong, M. Belić, and T. Huang, Three-dimensional finite-energy Airy self-accelerating parabolic-cylinder light bullets, *Phys. Rev. A* **88**, 033824 (2013).
- [19] D. N. Christodoulides, N. K. Efremidis, P. Di Trapani, and B. A. Malomed, Spatiotemporal Airy-Bessel bullets, *Opt. Lett.* **29**, 1446 (2004).
- [20] M. S. Mills, G. A. Siviloglou, N. Efremidis, T. Graf, E. M. Wright, J. V. Moloney, and D. N. Christodoulides, Localized waves with spherical harmonic symmetries, *Phys. Rev. A* **86**, 063811 (2012).
- [21] D. Zwillinger, *Handbook of Differential Equations*, 3rd ed. (Academic Press, Boston, 1997).
- [22] W.-P. Zhong and L. Yi, Two-dimensional Laguerre-Gaussian soliton family in strongly nonlocal nonlinear media, *Phys. Rev. A* **75**, 061801(R) (2007).
- [23] W.-P. Zhong, M. Belić, and T. Huang, Three-dimensional Bessel light bullets in self-focusing Kerr media, *Phys. Rev. A* **82**, 033834 (2010).
- [24] M. Belić, N. Petrovic, W.-P. Zhong, R.-H. Xie, and G. Chen, Analytical Light Bullet Solutions to the Generalized (3+1)-Dimensional Nonlinear Schrödinger Equation, *Phys. Rev. Lett.* **101**, 123904 (2008).